MULTI-TARGET DETECTION WITH THE GENERALIZED METHOD OF MOMENTS

Ye'Ela Shalit[†]*, Ran Weber[†]*, Asaf Abas[‡]*, Shay Kreymer[†]*, and Tamir Bendory[†]

[†]School of Electrical Engineering, Tel Aviv University, Tel Aviv, Israel
[‡]Department of Applied Mathematics, Tel Aviv University, Tel Aviv, Israel

ABSTRACT

We consider the one-dimensional multi-target detection (MTD) problem of recovering a target signal from a noisy measurement that contains multiple copies of the signal, each randomly translated. Motivated by the structure reconstruction problem in single-particle cryo-electron microscopy, we focus on the high noise regime, where the noise hampers accurate detection of the signal occurrences. We develop a generalized method of moments framework to estimate the image directly from a measurement, and compare the framework to the method of moments through numerical experiments. We demonstrate signal recovery in highly noisy environments, and prove numerically the optimality of the generalized method of moments.

Index Terms— Autocorrelation analysis, generalized method of moments, multi-target detection, cryo-electron microscopy.

1. INTRODUCTION

We study the multi-target detection (MTD) problem of estimating a target signal $x \in \mathbb{R}^L$ from a noisy measurement that contains multiple copies of the signal, each randomly translated [1], [2], [3], [4], [5], [6]. Specifically, let $y \in \mathbb{R}^N$ be a measurement of the form

$$y[\ell] = \sum_{i=1}^{p} x[\ell - \ell_i] + \varepsilon[\ell], \qquad (1)$$

where $\{\ell_i\}_{i=1}^{p} \in \{L+1, \ldots, N-L\}$ are arbitrary translations, and $\varepsilon[\ell] \overset{i.i.d.}{\sim} \mathcal{N}(0, \sigma^2)$. The translations and the number of occurrences of x in y are unknown. Figure 1 presents examples of a measurement y at different signal-to-noise ratios (SNRs). We define SNR $:= \frac{\|x\|_2^2}{L\sigma^2}$. [Asaf: The definition of the SNR isn't relevant here - I think it would be better at numerical exp']

The MTD model serves as a mathematical abstraction of the cryo-electron microscopy (cryo-EM) technology for
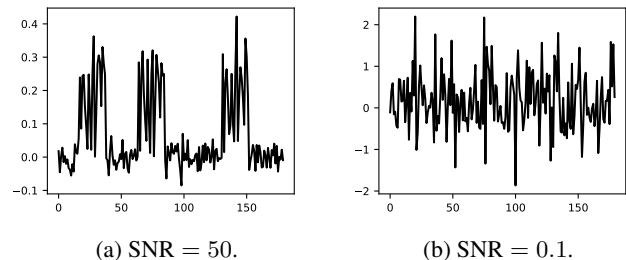
Fig. 1: Two measurements at different noise levels: SNR = 50 (left); SNR = 0.1 (right). Each measurement contains multiple copies of the target signal. Our goal is to estimate the target signal directly from y.

macromolecular structure determination [7], [8], [9]. In a cryo-EM experiment [10], biological macromolecules suspended in a liquid solution are rapidly frozen into a thin ice layer. An electron beam then passes through the sample, and a two-dimensional tomographic projection is recorded. Importantly, the 2-D location and 3-D orientation of particles within the ice are random and unknown. This measurement, called *micrograph*, is further affected by high noise levels and the optical configuration of the microscope.

In the current analysis workflow of cryo-EM data [11], [12], [13], the 2-D projections are first detected and extracted from the micrograph, and later rotationally and translationally aligned to reconstruct the 3-D molecular structure. This approach fails for small molecules, which induce low contrast, and thus low SNR. This makes them difficult to detect and align [6], [7], [11], [14], rendering current cryo-EM algorithmic pipeline ineffective. For example, in the limit SNR $\to$ 0, reliable detection of signals' locations within the measurement is impossible [6, Proposition 3.1]. In this work, we focus on the low SNR regime (e.g., panel (b) in Figure 1) in which the signal occurrences are swamped by the noise, and the locations of the signal occurrences cannot be detected reliably.

The MTD model was devised in [6] in order to study the recovery of small molecules directly from the micrograph, below the current detection limit of cryo-EM [7], [15]. An autocorrelation analysis technique (see Section 2.1) was implemented to recover low-resolution 3-D structures from noise-

less simulated data under a simplified model. Autocorrelation analysis consists of finding a signal that best explains the empirical autocorrelations of the measurement, by minimizing a least-squares (LS) objective. For any noise level, those autocorrelations can be estimated to any desired accuracy for sufficiently large N. Computing the autocorrelations is straightforward and requires only one pass over the data, which is advantageous for massively large datasets, such as cryo-EM datasets [11].

Autocorrelation analysis is a variation of the method of moment (MoM), which is a classical statistical inference technique, tracing back to 1894 [16]. This work studies the application of the *generalized method of moments* (GMM) application into the MTD problem. The GMM theory, which was first introduced in [17], shows that the GMM provides an optimal estimator, in comparison with other weighted LS objective function. Previous work shows that the GMM suggests a significant improvement, e.g., [19], [20], and specifically in cryo-EM [18].

The main contribution of this paper is in extending the MoM framework introduced in [1] by developing a GMM framework for the one-dimensional MTD problem. We devise an algorithm for the recovery of the target signal from a measurement, and demonstrate a successful reconstruction in noisy regimes (see Section 3). Moreover, we conduct numerical experiments which demonstrate the algorithm superiority. It is thus a step towards efficiently estimating a molecular structure directly from a noisy cryo-EM micrograph [6].

2. MATHEMATICAL FRAMEWORK

2.1. Autocorrelation analysis

The autocorrelation of order q of a signal $z \in \mathbb{R}^N$ is defined as

$$A_z^q[\ell_1, \ldots, \ell_{q-1}] := \mathbb{E}_z \left[\frac{1}{N} \sum_{i \in \mathbb{Z}} z[i]z[i+\ell_1] \cdots z[i+\ell_{q-1}] \right],$$

where $\ell_1, \ldots, \ell_{q-1}$ are integer shifts. Indexing out of bounds is zero-padded, that is, $z[i] = 0$ out of the range $\{0, \ldots, N-1\}$. In this work, we use the first three autocorrelations.

As N grows indefinitely, the empirical autocorrelations of z almost surely (a.s.) converge to the population autocorrelations of z:

$$\lim_{N \to \infty} \frac{1}{N} \sum_{i \in \mathbb{Z}^2} z[i]z[i+\ell_1] \cdots z[i+\ell_{q-1}] \stackrel{\text{a.s.}}{=} A_z^q[\ell_1, \ldots, \ell_{q-1}],$$

by the law of large numbers.

Our goal is to relate the autocorrelations of the measurement with the target signal x. In particular, the first-order autocorrelation is defined as

$$A_y^1 := \frac{1}{N} \sum_{i \in \mathbb{Z}} y[i].$$

This is the mean of the measurement. The second-order autocorrelation of y, $A_y^2 : \mathbb{Z} \to \mathbb{R}$, is defined by

$$A_y^2[\ell_1] := \frac{1}{N} \sum_{i \in \mathbb{Z}} y[i]y[i+\ell_1],$$

and the third-order autocorrelation $A_y^3 : \mathbb{Z} \times \mathbb{Z} \to \mathbb{R}$ by

$$A_y^3[\ell_1, \ell_2] := \frac{1}{N} \sum_{i \in \mathbb{Z}} y[i]y[i+\ell_1]y[i+\ell_2].$$

2.2. Autocorrelations under the well-separated model

We discuss the well-separated case of the MTD problem, which was studied in [1]. In this case, we assume that each signal in the measurement y is separated by at least a full signal length from its neighbors. Specifically, we assume that

$$|\ell_{i_1} - \ell_{i_2}| \geq 2L - 1, \quad \text{for all } i_1 \neq i_2.$$

To compute the third-order autocorrelation (2.1), we compute the product of y with its two shifts. Importantly, for ℓ-s in the range $\mathcal{L} = \{0, \ldots, L-1\}$, any given occurrence of x in y is only ever correlated with itself, and never with another occurrence.

In [1], it was shown that under the separation condition (2.2), for any fixed level of noise σ^2, density γ and signal length L, in the limit $N \to \infty$ we have that

$$A_y^1 \stackrel{\text{a.s.}}{=} \gamma A_x^1, \tag{2}$$

$$A_y^2[\ell_1] \stackrel{\text{a.s.}}{=} \gamma A_x^2[\ell_1] + \sigma^2 \delta[\ell_1], \tag{3}$$

$$A_y^3[\ell_1, \ell_2] \stackrel{\text{a.s.}}{=} \gamma A_x[\ell_1, \ell_2]$$
$$+ \gamma A_x^1 \sigma^2 (\delta[\ell_1] + \delta[\ell_2] + \delta[\ell_1 - \ell_2]), \tag{4}$$

for $\ell_1, \ell_2 \in \mathcal{L}$, where

$$\delta[\ell] = \begin{cases} 1 \text{ if } \ell = \vec{0}, \\ 0 \text{ otherwise}, \end{cases}$$

is the Kronecker delta function. Here, γ is the density of the target images in the measurement and is defined by

$$\gamma = p \frac{L}{N}.$$

As such, (2) - (4) relate the autocorrelations of the measurement with those of the target signal x. Importantly, the aforementioned relations between the autocorrelations of y and x do not directly depend on the location of individual signal occurrences in the measurement, but only through the density parameter γ. Therefore, detecting the signal occurrences is not a prerequisite for signal recovery, and thus signal recovery is possible even in very low SNR regimes.

Next, we introduce the following notations

$$\mathcal{A}_y^1 := A_y^1, \quad \mathcal{A}_x^1 := \gamma A_x^1, \quad \mathcal{A}_y^2 := \left\{ A_y^2[\ell] \right\}_{\ell=0}^{L-1},$$

$$\mathcal{A}_x^2 := \left\{ \gamma A_x^2[\ell] + \sigma^2 \delta[\ell] \right\}_{\ell=0}^{L-1}, \quad \mathcal{A}_y^3 := \left\{ A_y^3[\ell_1, \ell_2] \right\}_{\ell_1, \ell_2=0}^{L-1},$$

$$\mathcal{A}_x^3 := \Big\{ \gamma A_x^3[\ell_1, \ell_2]$$

$$+ \gamma A_x^1 \sigma^2 (\delta[\ell_1] + \delta[\ell_2] + \delta[\ell_1 - \ell_2]) \Big\}_{\ell_1, \ell_2=0}^{L-1}.$$

2.3. Signal recovery from autocorrelations

Following [1], [2], [3], [4], [5] and based on the notations presented above, we formulate a non-convex least squares problem for estimating the signal x and the density γ from the autocorrelations of the measurement y:

$$\min_{x,\gamma>0} w_1 (\mathcal{A}_y^1 - \mathcal{A}_x^1)^2$$
$$+ w_2 \|\mathcal{A}_y^2 - \mathcal{A}_x^2\|_2^2 + w_3 \|\mathcal{A}_y^3 - \mathcal{A}_x^3\|_2^2, \quad (5)$$

where the weights were chosen such that each term is equally weighted, as suggested by [1]. This LS estimator serves as a benchmark to the GMM estimator, which is developed in the following section.

2.4. Generalized method of moments

2.4.1. The GMM framework

In its most simplified form, the GMM generalizes (5) by replacing the LS objective with specific optimal weights. This choice guarantees favorable asymptotic statistical properties, such as the minimal asymptotic variance of the estimation error.

Let us define the *moment function*, $f(\theta, y)\colon \Theta \times \mathbb{R}^r \to \mathbb{R}^q$. The moment function is chosen such that its expectation value is zero only at a single point $\theta = \theta_0$. Namely,

$$\mathbb{E}[f(\theta, y)] = 0 \quad \text{if and only if} \quad \theta = \theta_0. \quad (6)$$

The moment function must satisfy this uniqueness condition (6) and a few additional regularity conditions (which can be found in [17], [18]). This flexibility enables the GMM to be applied to a wide range of problems, such as subspace estimation [19].

In order to define the moment function for the MTD problem, we first define the i-th observation from the signal y as follows:

$$y_i := [y[i], \ldots, y[i+L]].$$

The choice of the moment function $f(\cdot)$ must fulfill (6) using the defined samples y_i. The natural choice of $f(\cdot)$ is

$$f(\theta, y_i) := \begin{bmatrix} \mathcal{A}_x^1 - \mathcal{A}_{y_i}^1 \\ \mathcal{A}_x^2 - \mathcal{A}_{y_i}^2 \\ \mathcal{A}_x^3 - \mathcal{A}_{y_i}^3 \end{bmatrix}, \quad (7)$$

where $\theta := [x, \gamma]$. The estimated sample moment function is the average of f over N observations:

$$g_N(\theta) = \frac{1}{N} \sum_{i=1}^N f(\theta, y_i) = \begin{bmatrix} \mathcal{A}_x^1 - \mathcal{A}_y^1 \\ \mathcal{A}_x^2 - \mathcal{A}_y^2 \\ \mathcal{A}_x^3 - \mathcal{A}_y^3 \end{bmatrix}. \quad (8)$$

The GMM estimator is defined as the minimizer of the weighted LS expression

$$\hat{\theta}_N = \arg\min_{\theta \in \Theta} g_N(\theta)^T W_N g_N(\theta). \quad (9)$$

Here, W_N is a fixed positive semi-definite (PSD) matrix. Note that the LS estimator (5) is a special case of (9).

2.4.2. Large Sample Properties

Before presenting the statistical properties of the GMM, we fix notation. We denote by $\xrightarrow{p}$ and $\xrightarrow{d}$ convergence in probability and in distribution, respectively. Let

$$S := \lim_{N \to \infty} \text{Cov}\left[\sqrt{N} g_N(\theta_0) \right], \quad (10)$$

be the covariance matrix of the estimated sample moment function (8) at the ground truth θ_0. We denote by $\{W_N\}_{N=1}^\infty$ a sequence of PSD matrices which converges almost surely to a positive definite (PD) matrix W. Finally, the expectation of the Jacobian of the moment function at the ground truth θ_0 is denoted by $G_0 = \mathbb{E}\left[\partial f(\theta_0, y)/\partial \theta^T \right]$.

The large sample properties of the GMM estimator were derived in [17], and are presented in the following theorem. The regularity conditions for this theorem can be found in [17], [21], [18].

Theorem 2.1. *Under the regularity conditions, the GMM estimator satisfies:*

A. (Consistency) $\hat{\theta}_N \xrightarrow{p} \theta_0$.

B. (Asymptotic normality)

$$\sqrt{N}(\hat{\theta}_N - \theta_0) \xrightarrow{d} \mathcal{N}(0, MSM^T),$$

where $M = [G_0^T W G_0]^{-1} G_0^T W$.

C. (Optimal choice of a weighting matrix) *The minimum asymptotic variance of $\hat{\theta}_N$ is given by $(G_0^T S^{-1} G_0)^{-1}$ and is attained by $W = S^{-1}$.*

Theorem 2.1 provides a matrix W that guarantees a minimal asymptotic variance of the estimator's error. The covariance matrix S of (10), which plays a central role in Theorem 2.1, is required to be a PD matrix. Therefore, the moment function must be chosen so that S is full-rank. As in [18], we remove the repeating entries of f (that appear due to the inherent symmetries of the autocorrelations).

It is important to note that in practice, the ground truth θ_0 is unknown a priori, so we cannot use the optimal weighting matrix. However as suggested in [18], for our choice of the moment function (7), it is enough to apply the covariance on the empirical part,

$$\text{Cov}[g(\theta)] = \text{Cov}\left[\left[A_{y_i}^1; \mathcal{A}_{y_i}^2; \mathcal{A}_{y_i}^3\right]\right].$$

3. NUMERICAL EXPERIMENTS

In this section, we present numerical comparisons for the estimators which was described in Section 2, the MoM and GMM estimators. The optimization problem (5) was minimized using the Broyden-Fletcher-Goldfarb-Shanno (BFGS) algorithm, while ignoring the positivity constraint on γ (namely, treating it as an unconstrained problem). We measure the estimation error by

$$\text{relative error}(x) = \frac{\|x - x^*\|_2}{\|x^*\|_2},$$

where x^* is the true signal, and x is the estimated signal. The code to reproduce all experiments is publicly available at `https://github.com/krshay/MTD-GMM`.

3.1. Recovery error as a function of the measurement length

Figure 2 presents recovery error as a function of the measurement size, for a fixed noise level (SNR = 50). The measurements are generated according to (1) with density $\gamma = 0.2$. The target signals in the measurements are of length $L = 21$. We try to estimate the signal from 5 random initial guesses, and calculate the estimation error for the estimate whose final objective function is minimal. Then, we calculate the median error over 20 trials. As expected from the law of large numbers, both estimators' errors decay as $N^{-1/2}$. In addition, Theorem 2.1 provides the optimality of the GMM estimator over the MoM estimator, and indeed the median error of the GMM estimator is smaller than the error of the MoM estimator for all sizes. asafcI'm not sure if it is relevant to talk about the optimality here

3.2. Recovery error as a function of SNR

Next, we compared the recovery errors as a function of SNR, the results are in Figure 3. The signal length y is $N = 10^6$. As in Section 3.1, the measurements are generated according to (1) with density $\gamma = 0.2$, the target signals in the measurements are of length $L = 21$, and we try to estimate the signal from 5 random initial guesses and calculate the estimation error for the estimate whose final objective function is minimal. Then, we calculate the **median** over **20** trials.
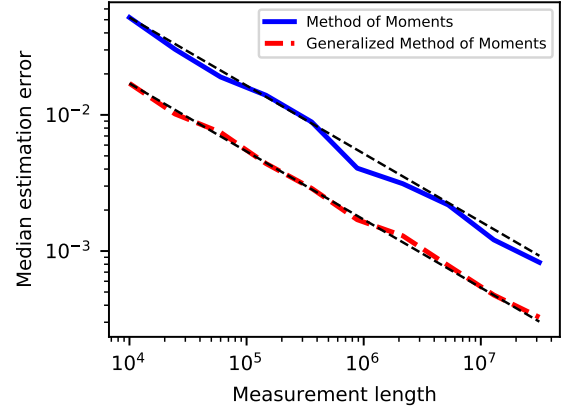
4. CONCLUSION

Fig. 2: The median estimation error of recovering the signal x, as a function of the measurement length N, by: (a) the MoM estimator; (b) the GMM estimator.
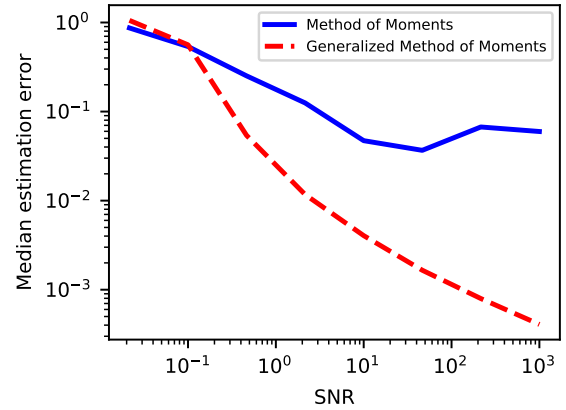

Fig. 3: Median estimation error of recovering the signal x, as a function of SNR, by: (a) the MoM estimator; (b) the GMM estimator.

5. REFERENCES

[1] Tamir Bendory, Nicolas Boumal, William Leeb, Eitan Levin, and Amit Singer, "Multi-target detection with application to cryo-electron microscopy," *Inverse Problems*, vol. 35, no. 10, pp. 104003, 2019.

[2] Ti-Yen Lan, Tamir Bendory, Nicolas Boumal, and Amit Singer, "Multi-target detection with an arbitrary spacing distribution," *IEEE Transactions on Signal Processing*, vol. 68, pp. 1589–1601, 2020.

[3] Nicholas F Marshall, Ti-Yen Lan, Tamir Bendory, and Amit Singer, "Image recovery from rotational and translational invariants," in *ICASSP 2020-2020 IEEE International Conference on Acoustics, Speech and Signal Processing (ICASSP)*. IEEE, 2020, pp. 5780–5784.

[4] Tamir Bendory, Ti-Yen Lan, Nicholas F Marshall, Iris Rukshin, and Amit Singer, "Multi-target detection with rotations," *arXiv preprint arXiv:2101.07709*, 2021.

[5] Shay Kreymer and Tamir Bendory, "Two-dimensional multi-target detection," *arXiv preprint arXiv:2105.06765*, 2021.

[6] Tamir Bendory, Nicolas Boumal, William Leeb, Eitan Levin, and Amit Singer, "Toward single particle reconstruction without particle picking: breaking the detection limit," *arXiv preprint arXiv:1810.00226*, 2018.

[7] Richard Henderson, "The potential and limitations of neutrons, electrons and X-rays for atomic resolution microscopy of unstained biological molecules," *Quarterly Reviews of Biophysics*, vol. 28, no. 2, pp. 171–193, 1995.

[8] Eva Nogales, "The development of cryo-EM into a mainstream structural biology technique," *Nature methods*, vol. 13, no. 1, pp. 24–27, 2016.

[9] Xiao-Chen Bai, Greg McMullan, and Sjors HW Scheres, "How cryo-EM is revolutionizing structural biology," *Trends in Biochemical Sciences*, vol. 40, no. 1, pp. 49–57, 2015.

[10] Joachim Frank, *Three-dimensional electron microscopy of macromolecular assemblies: visualization of biological molecules in their native state*, Oxford University Press, 2006.

[11] Tamir Bendory, Alberto Bartesaghi, and Amit Singer, "Single-particle cryo-electron microscopy: Mathematical theory, computational challenges, and opportunities," *IEEE Signal Processing Magazine*, vol. 37, no. 2, pp. 58–76, 2020.

[12] Sjors HW Scheres, "RELION: implementation of a Bayesian approach to cryo-EM structure determination," *Journal of Structural Biology*, vol. 180, no. 3, pp. 519–530, 2012.

[13] Ali Punjani, John L Rubinstein, David J Fleet, and Marcus A Brubaker, "cryoSPARC: algorithms for rapid unsupervised cryo-EM structure determination," *Nature methods*, vol. 14, no. 3, pp. 290–296, 2017.

[14] Cecilia Aguerrebere, Mauricio Delbracio, Alberto Bartesaghi, and Guillermo Sapiro, "Fundamental limits in multi-image alignment," *IEEE Transactions on Signal Processing*, vol. 64, no. 21, pp. 5707–5722, 2016.

[15] Edoardo D'Imprima and Werner Kühlbrandt, "Current limitations to high-resolution structure determination by single-particle cryoEM," *Quarterly Reviews of Biophysics*, vol. 54, 2021.

[16] Karl Pearson, "Contributions to the mathematical theory of evolution," *Philosophical Transactions of the Royal Society of London. A*, vol. 185, pp. 71–110, 1894.

[17] Lars Peter Hansen, "Large sample properties of generalized method of moments estimators," *Econometrica*, vol. 50, no. 4, pp. 1029, 1982.

[18] Asaf Abas, Tamir Bendory, and Nir Sharon, "The generalized method of moments for multi-reference alignment," *arXiv preprint arXiv:2103.02215*, 2021.

[19] Jianqing Fan and Yiqiao Zhong, "Optimal subspace estimation using overidentifying vectors via generalized method of moments," *arXiv preprint arXiv:1805.02826*, 2018.

[20] David Roodman, "How to do xtabond2: An introduction to difference and system GMM in stata," *The stata journal*, vol. 9, no. 1, pp. 86–136, 2009.

[21] Alastair R Hall, *Generalized method of moments*, Oxford university press, 2005.